

**THE REPUBLIC OF TURKEY  
BAHCESEHIR UNIVERSITY**

**AUTOMATIC SEGMENTATION OF CENTRAL  
SULCUS ON BRAIN MR IMAGES**

**Master's Thesis**

**OĐUZ DEMİR**

**ISTANBUL, 2013**

**THE REPUBLIC OF TURKEY  
BAHCESEHIR UNIVERSITY**

**GRADUATE SCHOOL OF NATURAL AND APPLIED  
SCIENCES  
COMPUTER ENGINEERING PROGRAM**

**AUTOMATIC SEGMENTATION OF CENTRAL  
SULCUS ON BRAIN MR IMAGES**

**Master's Thesis**

**OĐUZ DEMİR**

**THESIS ADVISOR: ASSIST. PROF. DR. DEVRİM ÜNAY**

**ISTANBUL, 2013**

**THE REPUBLIC OF TURKEY  
BAHCESEHIR UNIVERSITY**

**GRADUATE SCHOOL OF NATURAL AND APPLIED SCIENCES  
COMPUTER ENGINEERING PROGRAM**

Name of the thesis: Automatic Segmentation of Central sulcus on Brain MR images

Name/Last Name of the Student: Oğuz Demir

Date of the Defense of Thesis: 03 September 2013

The thesis has been approved by the Graduate School of Natural and Applied Sciences.

Assoc. Prof. Dr. , Tunç BOZBURA  
Graduate School Director  
Signature

I certify that this thesis meets all the requirements as a thesis for the degree of Master of Science.

Assoc. Prof. Dr., Tarkan AYDIN  
Program Coordinator  
Signature

This is to certify that we have read this thesis and we find it fully adequate in scope, quality and content, as a thesis for the degree of Master of Science.

| <u>Examining Comittee Members</u>                   | <u>Signature</u> |
|---|------------------|
| Thesis Supervisor<br>Assist. Prof. Dr., Devrim UNAY | -----            |
| Member<br>Assoc.Prof. Dr., Çiğdem EROĞLU ERDEM      | -----            |
| Member<br>Assoc. Prof. Dr., Kamuran Kadıpaşalıoğlu  | -----            |

## ACKNOWLEDGEMENTS

First and foremost I would like to thank my master thesis advisor Assist. Prof. Dr. Devrim Ünay for his priceless guidance and support in every phase of my study. I appreciate very much for his all helpful recommendations, reviews and invaluable advices. I will never forget his patience and belief in me during my study. He has been a great advisor to me for this study and beyond.

I am thankful to my thesis committee members, Assoc.Prof. Dr. Çiğdem Erođlu Erdem and Assoc. Prof. Dr. Kamuran Kadıpaşalıođlu, for their invaluable feedbacks about my study and best wishes for my future.

I would also like to thank to my wife Neşe for her entire support, reviews and understanding during my project.

Finally I would like to thank Bahcesehir University for accepting me and supporting throughout my graduate education.

Oguz Demir

## ABSTRACT

### AUTOMATIC SEGMENTATION OF CENTRAL SULCUS ON BRAIN MR IMAGES

Oğuz Demir

Computer Engineering Program

Thesis Supervisor: Assist. Prof. Dr. Devrim Ünay

September 2013, 39 Pages

Exploring structural relationship between dementia diseases and the brain itself and its structures is a new area of research. In literature; there are several studies which deal with defining, labeling and segmenting anatomical structures of the brain on MR images. However, when the number of the published paper is taken into consideration; it can be said that reviewing this relationship between dementia diseases and Central Sulcus, which is one of the most important sulcal structure in brain, is a new research area. It is also important to segment and retrieve volumetric information of central sulcus since it has been used to visually grade to dementia level.

There are many software and tools that allow users to make segmentations and comparisons over MR images, but most of them are not capable of producing accurate segmentation of a specific region of the brain (e.g. central sulcus), automatically. Alternatively, these operations can be done by selecting the region under investigation manually. Yet, this manual procedure is not preferred since it is error-prone and time consuming.

In this project, it is aimed to develop a methodology to segment central sulcus regions over brain MR images, without any human intervention, and export this segmentation information as a reusable data.

The test dataset, which is used in this study, contains various levels of atrophy besides different contrasts and resolutions. In this respect, this study provides a generic methodology for central sulcus segmentation on brain MR images, taken from routine clinical practice, independent of image quality or other deformations based on atrophy in brain.

**Key Words:** Central Sulcus, Detection, Segmentation, MRI, Atlas Mapping, Registration, Region Growing, Brain Extraction, AC-PC line detection

## ÖZET

### BEYİN MR GÖRÜNTÜLERİ ÜZERİNDE OTOMATİK CENTRAL SULCUS AYRIŞTIRMASI

Oğuz Demir

Bilgisayar Mühendisliği Programı

Tez Danışmanı: Yrd. Doç. Dr. Devrim Ünay

Haziran 2013, 39 Sayfa

Demans hastalıkları ile beyin arasındaki yapısal ilişkilerin araştırılması yeni sayılabilecek araştırma konularından birisidir. Bu çerçevede, beyin üzerindeki yapıların MR görüntüleri üzerinde tanımlanması, isimlendirilmesi ve ayrıştırılması ile ilgili çalışmalar literatürde bulunmaktadır. Ancak bu tür yapısal ilişkilerin beyin önemli sulkal yapılarından biri olan Central sulcus üzerinden tespit edilmeye çalışılması, literatürdeki çalışma sayısının azlığı göz önünde bulundurulduğunda yeni bir çalışma alanı olarak görülebilir.

MR görüntüleri üzerinde; çeşitli ayrıştırma, karşılaştırma operasyonlarının kullanıcılar tarafından yapılabilmesini sağlayan araçlar ve yazılımlar bulunmaktadır ancak bu araç ya da yazılımlarda beyin özellikle ayrıştırılması istenen bölümlerini otomatik biçimde ayrıştırabilme yeteneği bulunmamaktadır. Bu alanların el ile ayrıştırılması ise hataya açık olması ve zaman tüketen işlemler olması nedeni ile tercih edilmemektedir.

Bu çalışmanın amacı, kullanıcı etkileşimi olmadan, verilen beyin MR görüntüleri üzerinde Central Sulcus yapısının tespit edilmesi ve yeniden kullanılabilir veri olarak dışa aktarılabilmesinin sağlanmasıdır.

Bu çalışma sırasında kullanılan test veri seti, farklı çözünürlükte ve keskinlik değerlerine sahip verilerin yanında farklı demans derecelendirmelerine sahip hasta verileri içermektedir. Bu bağlamda geliştirilen yöntem, günlük klinik çalışmalar sonucu elde edilen MR görüntüleri üzerinde; çözünürlük, demans temelli deformasyon ve imaj keskinliğinden bağımsız olarak çalışabilen bir çözüm olması anlamında önemlidir.

**Anahtar Kelimeler:** Central Sulcus, Segmentation, MRI, Atlas Mapping, Registration, Region Growing, Brain Extraction, AC-PC line detection

## CONTENTS

|   |             |
|---|-------------|
| <b>TABLES</b> .....   | <b>viii</b> |
| <b>FIGURES</b> .....  | <b>ix</b>   |
| <b>ABBREVIATIONS</b> .....                                  | <b>x</b>    |
| <b>INTRODUCTION</b> .....                                   | <b>1</b>    |
| <b>1. LITERATURE REVIEW</b> .....                           | <b>5</b>    |
| <b>2.1 ANATOMICAL RESEARCH</b> .....                        | <b>5</b>    |
| <b>2.2 CS AND OTHER SULCAL STRUCTURE SEGMENTATION</b> ..... | <b>8</b>    |
| <b>2. METHODS</b> .....                                     | <b>11</b>   |
| <b>3.1 SLICE SELECTION</b> .....                            | <b>11</b>   |
| <b>3.2 ATLAS GENERATION</b> .....                           | <b>16</b>   |
| <b>3.3 ATLAS MAPPING AND SEED POINT SELECTION</b> .....     | <b>18</b>   |
| <b>3.4 SEGMENTATION</b> .....                               | <b>20</b>   |
| <b>3. RESULTS</b> .....                                     | <b>23</b>   |
| <b>4.1 SLICE SELECTION</b> .....                            | <b>23</b>   |
| <b>4.2 ATLAS MAPPING</b> .....                              | <b>26</b>   |
| <b>4.3 SEGMENTATION</b> .....                               | <b>28</b>   |
| <b>4. DISCUSSIONS AND RESULTS</b> .....                     | <b>35</b>   |
| <b>5.1 RESULTS</b> .....                                    | <b>36</b>   |
| <b>5.2 FUTURE WORKS</b> .....                               | <b>38</b>   |
| <b>REFERENCES</b> .....                                     | <b>40</b>   |

## TABLES

|   |    |
|---|----|
| Table 4.1.1: Slice Selection Results.....                           | 24 |
| Table 4.3.1: Results for dynamic height measuring.....              | 30 |
| Table 4.3.2: Results for brain masking with BET.....                | 31 |
| Table 4.3.3: Results for brain masking with erosion operation ..... | 32 |
| Table 4.3.4: Results for manual slice selection.....                | 32 |



## FIGURES

|  |    |
|--|----|
| Figure 1.1: Sulci .....  | 1  |
| Figure 1.2: Sulcal structures in human brain .....   | 2  |
| Figure 1.3: MR imaging planes.....   | 3  |
| Figure 2.1: Image of CS .....  | 6  |
| Figure 2.2: Location of AC and PC .....  | 6  |
| Figure 2.3: CS Location above LV .....   | 7  |
| Figure 2.4: Statistical distribution of CS between AC and PC .....   | 8  |
| Figure 3.1.1: An image stack .....   | 11 |
| Figure 3.1: Lateral Ventricles .....   | 13 |
| Figure 3.2: Maximum Slice .....  | 15 |
| Figure 3.2.1: Example data with different atrophy levels. More atrophic case is seen on<br>the right. .... | 16 |
| Figure 3.2.2: Registration phase of atlas image generation. ....   | 17 |
| Figure 3.2.3: Final atlas image.....   | 18 |
| Figure 3.3.1: Intensity profile of a brain axial MR image along a lateral line.....                        | 19 |
| Figure 4.2.2: An exemplary visual result of Atlas Mapping.....   | 26 |
| Figure 4.2.3: Final Atlas Image .....  | 27 |

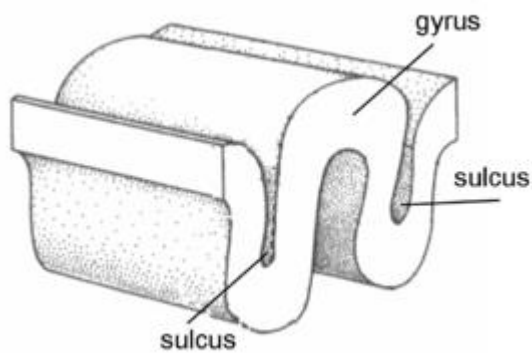
## ABBREVIATIONS

|               |   |   |
|---------------|---|---|
| CS            | : | Central Sulcus  |
| MRI           | : | Magnetic Resonance Imaging  |
| CSF           | : | Cerebrospinal Fluid   |
| AC            | : | Anterior Commissure   |
| PC            | : | Posterior Commissure  |
| Key Slice     | : | A slice on the Central Sulcus can be seen with its characteristic inverted omega shape. |
| Maximum Slice | : | A slice has maximum count of pixels within MRI slices.                                  |
| MSP           | : | Midsagittal Plane   |
| Voxel         | : | Volumetric Pixel  |
| CSF           | : | Cerebrospinal Fluid   |

## INTRODUCTION

In neuroanatomy, sulcus (plural form: sulci) term is used to define depressions or fissures in the brain surface. Although there are many different fissures in human brain, sulcus is mostly used for fissures that separate brain lobes from each other.

**Figure 1.1: Sulci**

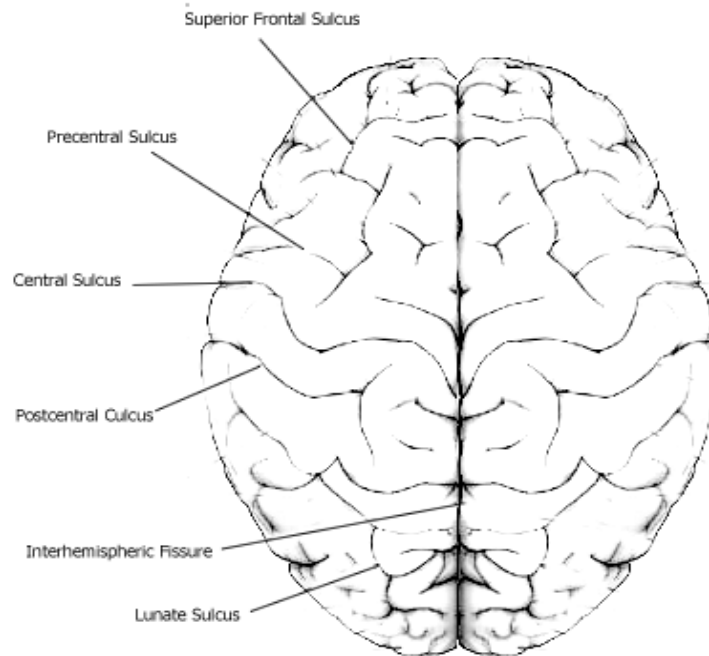


*Source: Wikipedia*

Fourteen sulci structures are defined in the human brain so far (Ono 1990). Those are; Interhemispheric Fissure, Sylvian Fissure, Parieto-occipital Fissure, Collateral Sulcus, Central Sulcus, Calcarine Sulcus, Superior Frontal Sulcus, Inferior Frontal Sulcus, Postcentral Sulcus, Intraparietal Sulcus, Superior Temporal Sulcus, Inferior Temporal Sulcus, Cingulate Sulcus, Precentral Sulcus.

Some of the main fissures can be seen on Figure 1.2

**Figure 1.2: Sulcal structures in human brain**



Identifying central sulcus in the human brain is important since it separates the Frontal Lobe, which is controlling emotion and decision mechanisms and the Parietal Lobe, which is processing sensor signals (e.g. touch, and taste) coming from human body. Central sulcus is the only sulcal structure in cerebral cortex that separates the two lobes from each other (Naidich and Brightbill 1996).

Central sulcus is an important landmark which separates the sensory region from the motor area. Since it has a characteristic shape, which will be described later in the slice selection chapter, location and shape of the central sulcus have been also used to identify other brain structures (Romstock, 2002)

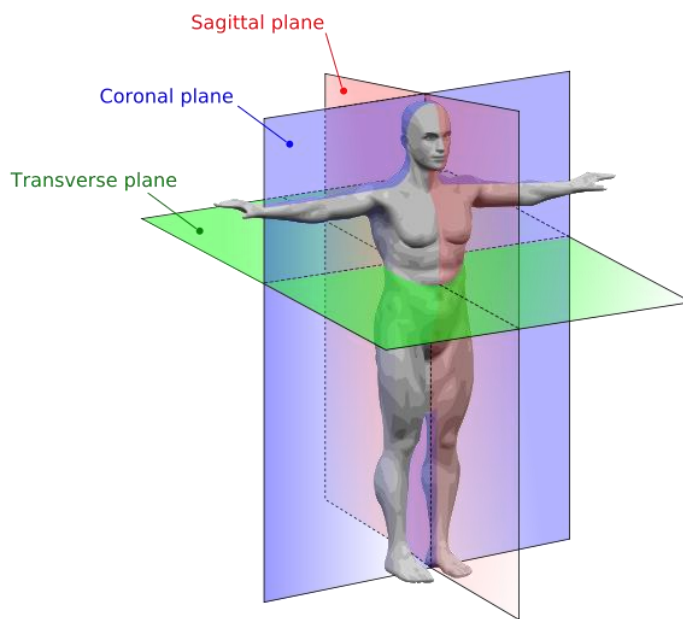
It is also important to investigate physical attributes of the Central sulcus to diagnose and grade dementia diseases (Barkhof, 2012). Some brain surgery and treatments (e.g.

epilepsy surgeries) have been planned by referring to the location of central sulcus (Romstock, 2002).

In this study, we worked on brain MR images to automatically identify and segment Central sulcus regions. MR Imaging is one of the visualization techniques used in radiology, which is capable of creating more detailed images than other modalities like X-ray and is suitable for medical image processing.

MR images can be taken in three different planes (Figure 1.3); sagittal plane (vertical plane divides body into left and right parts), coronal plane (vertical plane divides body into front and back parts) and axial (transverse) plane (horizontal plane divides body into upper and lower parts).

**Figure 1.3: MR imaging planes**



*Source: My-MS.org*

We aimed to develop a methodology, which segments central sulcus in brain MR images without any human intervention. Entire project was developed with Java programming language and implemented as a standalone ImageJ plugin. The reason why Java is preferred is that it is a cross platform, high performance, object oriented language. Also ImageJ is a popular, open source image processing platform developed using Java. All the tests and development were made with a MacBook Pro i5 computer in Mac OS X 10.7 operating system. ImageJ and other java applications have been run on Oracle Java v.1.7.

For ImageJ plugin development and debugging, IBM Eclipse Juno edition have been used.

The outline of this thesis is as follows.

In section 2, literature survey and anatomical research about Central sulcus will be summarized.

In section 3, implementation of the methodology will be discussed in three main parts as slice selection, atlas mapping and segmentation. In slice selection, a new methodology to find the slice that best displays the Central sulcus will be explained in detail. An atlas based registration technique for MR images, and a seed point detection approach (to be used in segmentation) will be covered in the atlas mapping part. Segmentation of Central sulcus and morphological operations used to improve the quality of the results are detailed in segmentation section.

In Section 4, results of this study will be given in relevant chapters with details and numeric values.

In Section 5, discussions about weaknesses, limitations and potential future works for the algorithm will take the place.

# 1. LITERATURE REVIEW

## 2.1 ANATOMICAL RESEARCH

Development of sulci and gyri structures in the human brain starts around 5<sup>th</sup> month before birth. While the brain continues to grow in the skull, it starts folding in and out. As a result; lobes, hemispheres, sulci, and gyri structures appear.

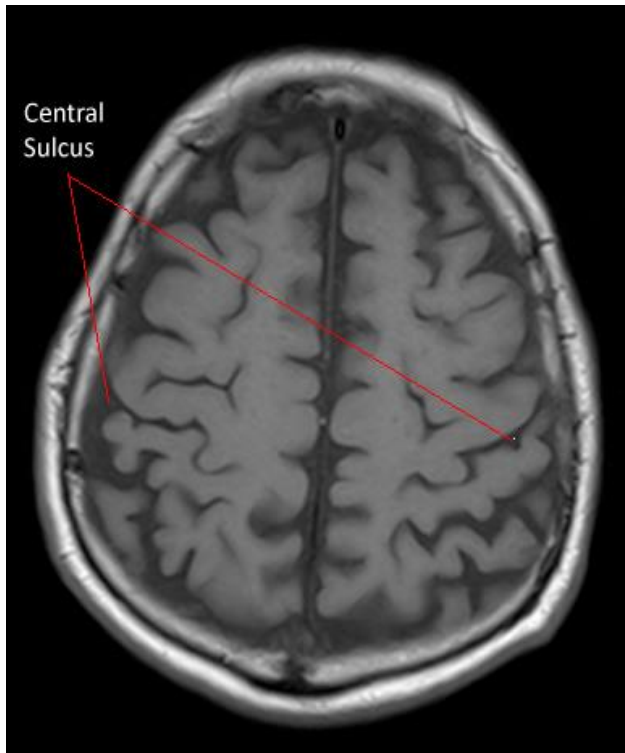
The Central Sulcus, also called Rolandic fissure after Luigi Rolando – an Italian anatomist, is one of those fissures in the cortex of human brain.

The Central sulcus is an important mark of the brain, separating the Parietal and Frontal Lobes from each other. Physical attributes of the Central sulcus (like depth, length etc.) are used by neurologists and radiologists to diagnose and grade level of dementia diseases.

Some fissure and sulci structures, like Interhemispheric Fissure, can be easily spot in human brain MR images. However, it is not the same for the central sulcus identification and segmentation of which may require a bit more effort.

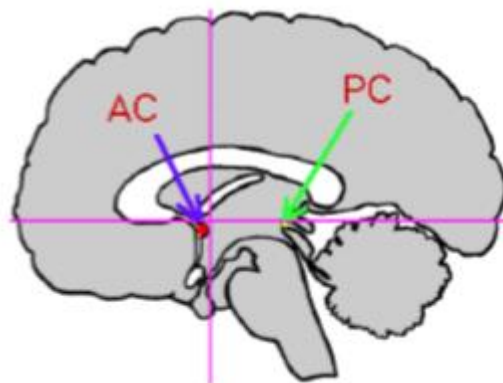
The easiest way of finding Central sulcus is examining the axial slices (Wei, 2004) In the human brain, the Central sulcus can be detected via its characteristic shape (inverted omega) visible at around 60mm below the top of the skull.

**Figure 2.1: Image of CS**



Central sulcus can also be pinpointed from the sagittal view, where between the Anterior and Posterior Commissures (Wei, 2004) (Figure 2.2). AC and PC are bunch of nerve fibers connecting the two hemispheres across the midline (interhemispheric fissure).

**Figure 2.2: Location of AC and PC**

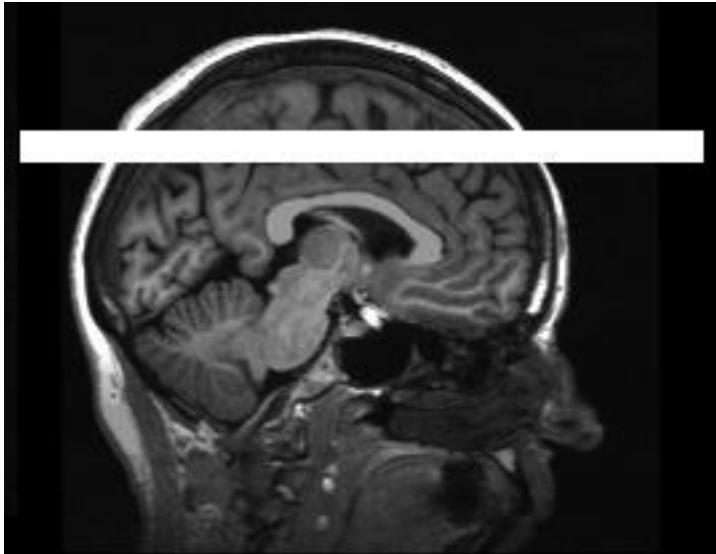


*Source: Wei (2008), Identification and Segmentation of the Central Sulcus from Human Brain MR Images*



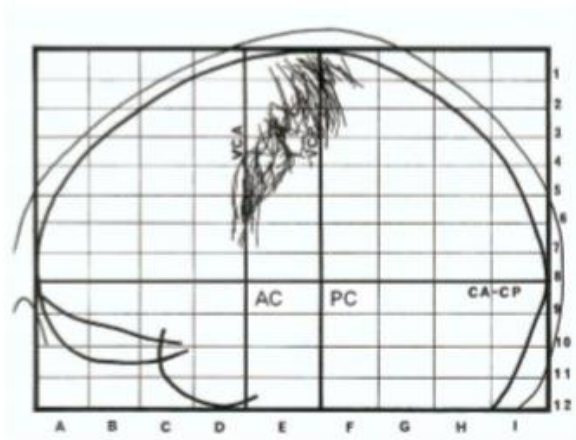
In the sagittal view, Central sulcus is located about 10-12 mm above the Lateral Ventricles. Ventricles are the holes which are filled with the CSF. Main functionality of those structures are protecting brain against traumas by increasing elasticity and creating a flowing system for the CSF. In Figure 2.3, white thick line defines the region where the Central sulcus can be seen in the sagittal view.

**Figure 2.3: CS Location above LV**



Like every other structure of the brain, physical attributes of Central sulcus vary from one individual to another. For example, statistical distribution regarding the location of CS derived from twenty different data sets (Wei, 2004) can be seen in Figure 2.4

**Figure 2.4: Statistical distribution of CS between AC and PC**



*Source: Wei (2004)*

To better understand CS, series of meetings were conducted with neurologists and radiologists from Bayındır Hospital Icerenkoy, Istanbul. The focus of these meetings was to understand the structural importance of Central sulcus and how it is located and analyzed by the doctors. Even for the experts, defining CS at only one MR slice is a confusing and demanding process. Thus, they prefer to track CS through additional slices and by examining its position in accordance with other known structures of the brain.

## **2.2 CS AND OTHER SULCAL STRUCTURE SEGMENTATION**

Central sulcus segmentation, especially automated methods, is a new subject for research. In literature, there are previous works but they are mostly related with general segmentation of sulcal structures. Those works are mostly semi-automated and make use of atlas or pattern based methodologies.

Some of those works are summarized below:

Behnke et al. 2003 proposed a methodology to find sulcal regions, containing gyri and sulcus structures, and classified them using a set of training data. First, sulcal structures are segmented using watershed algorithm and a region merging procedure based on two threshold values (one is related to the maximum height of the sulci and the other is related to the maximum distance between sulci and segmented regions).

Hayashi et al. 2010 presented a semi-automatic methodology, which starts at a manually given seed point, segments CSF to remove non brain tissue, and then generates a binary image using thinning to identify all the sulcal structures in the MR slices. In order to find CS within all sulcal structures previously found, it compares the result with a predefined statistical template.

Lohmann 2010 segmented sulcal structures on coronal MR images. First, he removed non brain tissue and generated a brain mask. Using morphological operations, a region boundary containing brain tissue was generated and brain mask was subtracted from this region. As a result, the remaining mask contains only sulcal structures. Finally, applying thinning algorithm gives the sulcal tree.

Wei 2004 worked on a automated CS segmentation method that makes use of anatomical information. The method detects slices that display AC-PC region, in a way which is not explained in the paper, and uses this slice as a reference, CS slice is found using a formulation.

$$N = (1 / 6 * N_{AC-PC}) + (2 / 5 * N_{TopTissue})$$

In this formulation  $N_{AC-PC}$  is the number of the slice where the AC-PC plane can be seen, and  $N_{TopTissue}$  is the slice number of the last slice where the brain tissue can be seen.

After detection of the slice that best displays CS, their 3D segmentation algorithm finds sulcal structures within a ROI defined by AC-PC lines at the sagittal plane. Finally, they detect CS by assuming that the largest sulci belong to the CS.

Wei's work is important, because it is the only fully automated method in the literature. However, there are obvious limitations of this method, as well as for the others. All of the methods, as argued in their original papers, work fine only on the condition that the images have high resolution with low noise level. Similarly, they need preprocessing, such as tissue segmentation or skull removing, before the identification and segmentation phases. This requirement largely affects the quality of the results, since many tissue segmentation and quantification techniques and tools do not work properly for every data set with varying acquisition details.

Above literature review reveals that to this date there is no robust solution for automated segmentation of central sulcus. Furthermore, even though some papers present results, validation information presented in most of the prior art is not enough. Besides, as software implementations of the prior art is missing, a quantitative comparison with the proposed solution was not possible.

A more thorough comparison between the results of this thesis and previous works is presented in the “Discussions and Results” section (Section 5).

## 2. METHODS

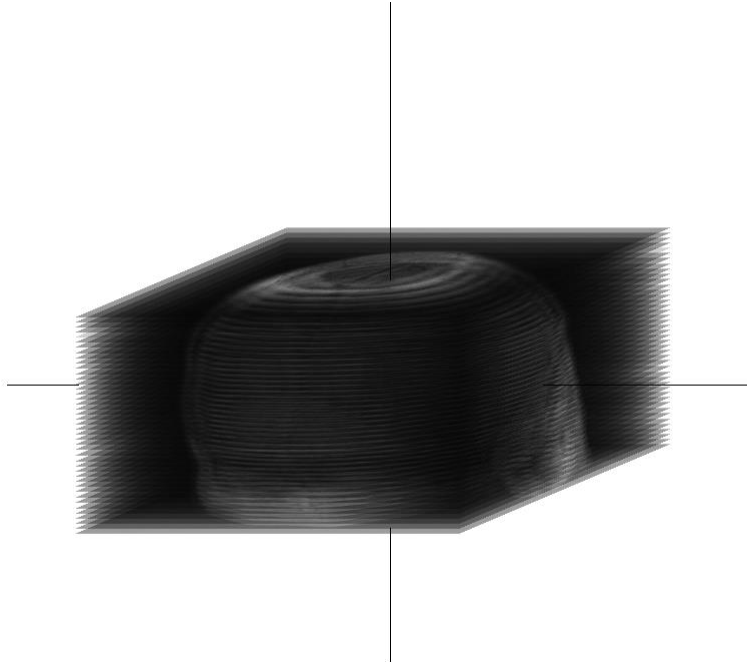
### 3.1 SLICE SELECTION

In medical image processing, especially for segmenting and labeling anatomical regions, Atlas Based methods are commonly used. An atlas can be defined as a combination of an intensity image (template) and a segmentation (labels). Brief information about atlas mapping and MR images is given here to clarify the importance of slice selection.

Despite the fact that MR images come in various formats (e.g. Analyze, Nifti, DICOM), basically an MR data is a stack of images that represents an object in 3D space (sometimes, in 4D space with the addition of time information).

In Figure 3.1.1, it can be seen how a 3D object is represented in a series of slices.

**Figure 3.1.1: An image stack**



In Atlas Based Segmentation technique, at first, atlas image must be registered over the target image. Then, segmentation image should be mapped (transformed) to the new

space identified in the registration stage. For the success of this methodology, the accuracy of registration and transformation is extremely important.

The atlas image, which is used in this project, was generated using the Key Slices, which were extracted from different data sets. It contains approximated location of the Central Sulcus and boundaries of the skull as well. Therefore, before mapping atlas over target image, it is important to find corresponding slices that the atlas image would be registered.

The slice which displaying Central Sulcus with its characteristic shape (inverted omega) can be seen in Figure 2.1. In the following pages, this slice will be called as “Key Slice”

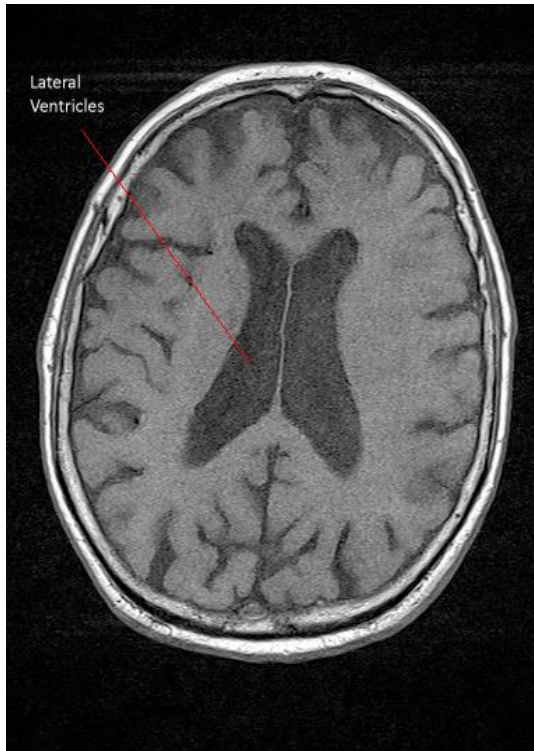
In order to find the key slice, different approaches has been applied.

First approach focused on segmenting Lateral Ventricles within MR image and using its location as a reference. In implementation, first, brain tissue is extracted using BET (Brain Extraction Toolkit), and then segmentation of Lateral Ventricles is completed.

BET is a popular, open source toolkit developed using C language. Main functionality of this tool is segmenting the brain tissue from MR images. Briefly, BET assumes that brain tissue is the largest closed component in an MR image. For extracting the brain tissue, first, it finds center of weight of the image and starts segmenting the brain tissue using clustering techniques.

After brain tissue is extracted using BET, in order to locate Lateral Ventricles fully automated ALVIN (Automatic Lateral Ventricle delineation) tool is used to segment the Lateral Ventricles from structural MR images. ALVIN assumes that Lateral Ventricles are the largest empty region close to the center of weight of the brain image. It finds seed points at Lateral Ventricle locations and segments Lateral Ventricles using region growing.

**Figure 3.1: Lateral Ventricles**



Anatomically, it is known that Central sulcus can be marked on axial images with its characteristic shape at 10-12 mm above of Lateral Ventricles. In this methodology, after the Lateral Ventricles are located, CS region is tracked through the top of the skull. The actual distance between Lateral Ventricles and Central sulcus is measured using the slice thickness information (resolution of the image along Z axis).

Dementia diseases at their later stages cause physical anomalies like atrophy (volume loss) in anatomical structures. Atrophy causes difficulties in both automated detection and segmentation of the brain structures. Also large slice thickness values (low resolution along Z axis) of MR images negatively affects the segmentation of lateral ventricles.

For increasing the quality of slice selection; relationship between MR image slices investigated as an alternative method.

First, simple thresholding operation is applied to the target image by using the mean intensity of the image as the threshold value. After this thresholding operation, pixels that have lower intensity values than the mean value of the image, are removed and the total count of the remaining pixels were computed for every slice. Therefore, the largest 2D

volume is found by selecting the slice with the highest total pixel count. In this thesis, this slice with the maximum pixel count is referred to as “Maximum Slice”.

To explore the relationship of maximum slice with other slices, total pixel count values are normalized with the total pixel count of the Maximum Slice. Table 3.1 displays an example from the database.

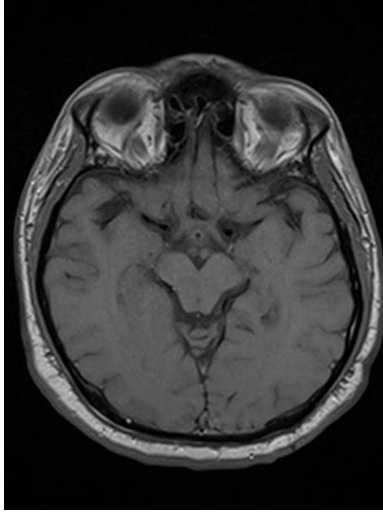
**Table 3.1**

| <b>Slice Number</b>             | <b>Pixel Count</b> | <b>Normalized Value</b> |
|---------------------------------|--------------------|-------------------------|
| Slice 16                        | 98037              | 0.95                    |
| Slice 17                        | 101818             | 0.99                    |
| <b>Slice 18 (Maximum Slice)</b> | <b>102833</b>      | <b>1</b>                |
| Slice 19                        | 101360             | 0.99                    |
| Slice 20                        | 101310             | 0.99                    |
| Slice 21                        | 101789             | 0.99                    |
| Slice 22                        | 101520             | 0.99                    |
| Slice 23                        | 101073             | 0.98                    |
| Slice 24                        | 99562              | 0.97                    |
| Slice 25                        | 98726              | 0.96                    |
| Slice 26                        | 97614              | 0.95                    |
| Slice 27                        | 95308              | 0.93                    |
| Slice 28                        | 92219              | 0.9                     |
| Slice 29                        | 89192              | 0.87                    |
| Slice 30                        | 85434              | 0.83                    |
| <b>Slice 31 (Key Slice)</b>     | <b>82976</b>       | <b>0.81</b>             |
| Slice 32                        | 79864              | 0.78                    |
| Slice 33                        | 76646              | 0.75                    |

Our observations revealed that the Maximum Slice almost always corresponds to the same slice level (displaying similar anatomical structures) across the data set, even in the extreme cases (atrophic brains, data with low resolution, or high noise).



**Figure 3.2: Maximum Slice**



Another pattern revealed in the results is that the normalized values of the Key Slices in the dataset fall in the 0.80 – 0.90 range when it is tracked through the top of the skull. As mentioned earlier, acquisition standard of MR images is not strict. So, the MR data can be flipped along the Z direction, and the top of the skull may be located at the first or last slice accordingly. Nevertheless, the proposed Key Slice selection method can handle such variations.

According to the slice thickness of the target image, one or more slices can be found within the 0.80 – 0.90 range. In such cases, slice selection is achieved by taking the average of the normalized values and finding the slice that has the closest normalized value to this average.

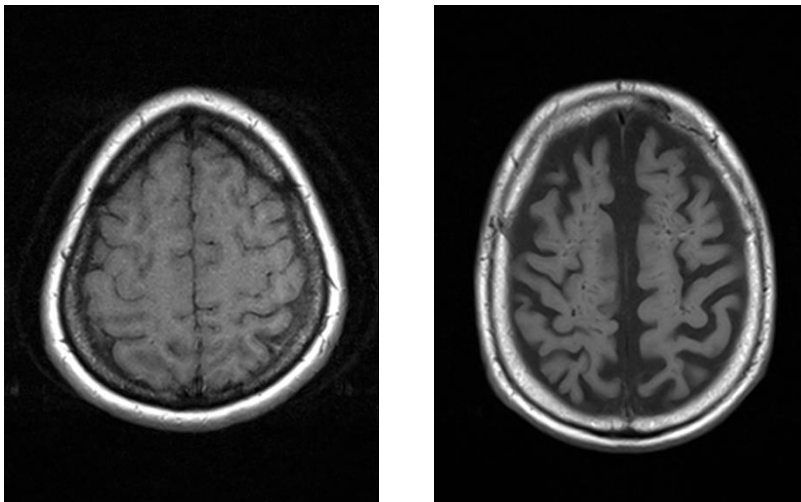
### 3.2 ATLAS GENERATION

Following slice selection, it is required to determine the approximate location of the CS and find seed points to initialize. Unfortunately, it is not easy to determine where the CS is located due to the variations in the brain structures of different individuals. Besides, pathologies like atrophy in the brain make it harder to solve this issue by magnifying dissimilarities and deformations in the brain. In order to minimize the negative effects of such issues, we decided to use an Atlas based approach to locate CS and create a ROI (region-of-interest) for segmentation.

In literature, various brain atlases marking different brain structures were presented. However, those atlases are not suitable for this work, since here we work with both healthy and pathological cases (atrophic brains).

For generation of the atlas, an anonymized MR dataset containing five cases (of 3 male and 2 female subjects from different age groups) with different levels of atrophy were acquired from Bayındır Hastanesi, İçerenköy. The data is visually graded with respect to atrophy level by a group of neurologists and radiologists from the same clinical site. In Figure 3.2.1, two examples from the data set, with different atrophy levels, can be seen.

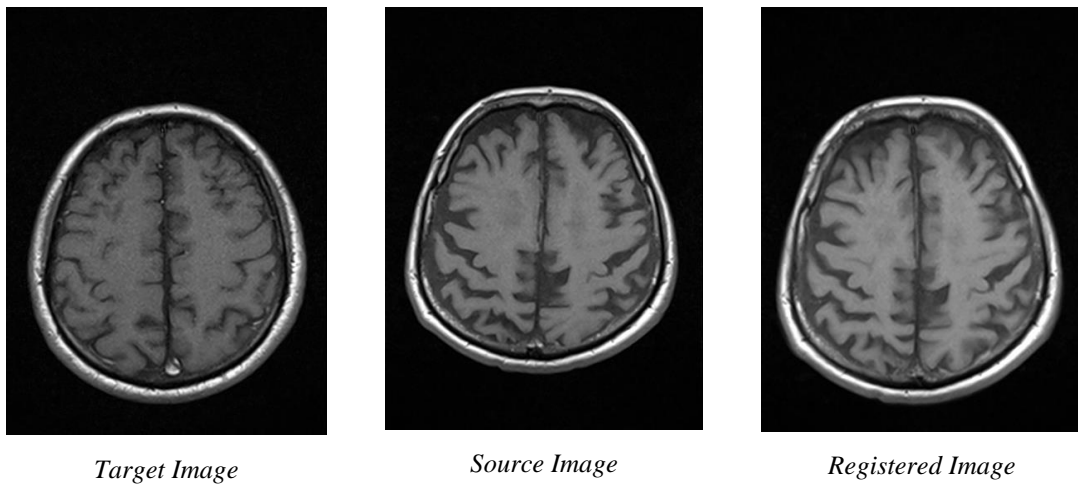
**Figure 3.2.1: Example data with different atrophy levels. More atrophic case is seen on the right.**



In order to map all data into the same space, one of the five data having a mid-level atrophy grade, has been selected as target image, while the others are linearly registered into the coordinate space of the target image using FSL/FLIRT(<http://fsl.fmrib.ox.ac.uk/fsl/fslwiki/>).

In Figure 3.2.2, a target image and a source image (before and after registration) can be seen. After registration, source image is scaled, skewed and rotated in order to match into the coordinate system of the target image.

**Figure 3.2.2: Registration phase of atlas image generation.**



After the registration phase, key slices (best displaying the inverted omega shape of the CS) were manually found and the central sulcus area is segmented manually in each hemispheres. Quality of this manual segmentation was then confirmed by the medical experts from Bayındır Hastanesi, Icerenkoy. The atlas image is then created by merging each manual segmentation result in a probabilistic way (if all manual segmentations contribute to a voxel, then that voxel will have highest probability of belonging to CS).

**Figure 3.2.3: Final atlas image.**



### **3.3 ATLAS MAPPING AND SEED POINT SELECTION**

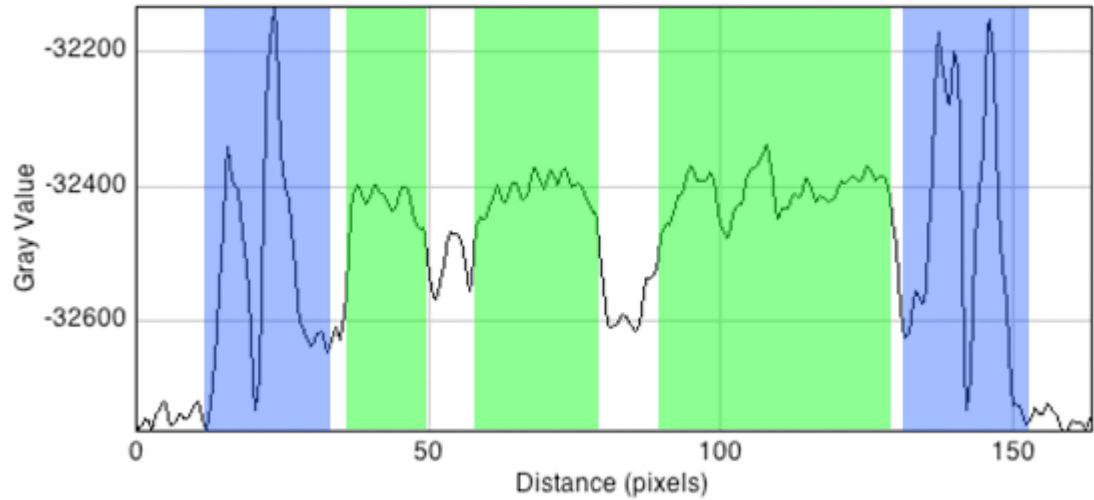
To identify the approximate location of central sulcus in the key slice of a new image, the atlas image must be further registered into the coordinate space of the new image. In this section, registration process of the atlas image into coordinate space of the new image will be explained.

For the atlas image registration, initially, FSL/FLIRT tool, which is previously used for the generation of atlas image, is tested. FSL/FLIRT is a tool that is optimized to work with complete 3D brain MR image stack, and it especially works well with high resolution data.

For registering atlas image over found slice, FLIRT should be used with proper parameters. Since it is optimized for full 3D images (containing entire slices), it failed in our slice-based registration problem (registration of a single-slice atlas image to a target slice).

Accordingly, a new registration methodology for registering single-slice atlas over brain MR image is developed. First step of the algorithm is automatically correcting the angular mismatch between atlas and target images. MR images can have  $\pm 15$  degrees in-plane rotation, because of the subject's head angle or movement. To correct this angle difference, first the hemispheric fissure line is found using a Ransac-based algorithm (Ekin, 2006), where intensity profiles along the lateral lines are examined. As it is seen in Figure 3.2.1, intensity values go up to high levels at the skull region (blue) while they are at almost constant value in the brain tissue area (green).

**Figure 3.3.1: Intensity profile of a brain axial MR image along a lateral line.**



Minimum values within this region mark the candidate points for hemispheric fissure. Then, a Ransac-based line fitting is realized on the candidate points.

Ransac algorithm starts with picking random two points within a data set, draws a line between these points, measures every other point's Euclidean distance to this line, and computes the sum of the distances (fitting error). It does this calculation for every possible point-pair, and identifies the line with the minimum error as the best fit.

After this step, angle of this line to the Y axis (i.e. rotation of the slice) is computed.

Secondly, algorithm finds height of the skull. For this, it uses intensity profile of the hemispheric fissure line, which is previously found. Similarly finds and marks the two maximums by searching from top to bottom and bottom to top, respectively. Distance between these two points defines the height of the skull.

Finally the algorithm draws a perpendicular line to the detected hemispheric fissure and crossing from its geometric center. This time, it runs a similar method to find and mark the left and the right bounds of the skull, and compute the width of the skull.

By using the rotation angle, width, and height of the skull, we create an affine transformation matrix, which we apply on the atlas image, and register it over the Key Slice.

At T1 weighted MR contrast, brain tissue and other living tissue can be seen brighter than other tissues like bones and fluids. For simple tissue segmentation, applying thresholding with a mean intensity value separates the tissue regions from the non-tissue area.

At the segmentation phase, the algorithm marks seed points by comparing atlas with the image underlying. First every pixel of the atlas is checked and for the positive pixels, underlying image's intensity value of the current pixel is checked. If the intensity value of pixel is lower than the mean value of the image, then is marked as seed point.

### **3.4 SEGMENTATION**

In this chapter, Central Sulcus segmentation techniques will be covered in detail. For segmentation of Central Sulcus, region growing technique (one of the most popular segmentation algorithm) has been used. Region growing algorithm starts with a given seed point and creates a region by adding appropriate neighbor points. Algorithm finishes region growing when there is no more points can be added into region.

Segmentation phase of the implementation can be covered in three main parts as “Preprocessing”, “Region Growing” and “Shape Closing”.

Depending on the shape of the Central Sulcus, atlas mapping section would generate multiple seed points at different locations. To increase quality of output and the performance, those seed points have been preprocessed before starting region growing.

In implementation of preprocessing phase, every seed points were processed and clusters were created with the neighborhood seed points. Then, for every cluster, average intensity value, which will be used as thresholding value in next steps, was computed.

In region growing phase, area of the each cluster were enlarged by using region growing technique. For every cluster, neighbor pixels around cluster processed and intensity values were compared with the average intensity value of the cluster. If the intensity value were equal or lower than the intensity value of the cluster, neighbor pixel is added into cluster and average intensity value of the cluster recomputed.

Region growing technique works well for only closed components. This limitation of the technique produces difficulties on segmenting brain structures since the brain structures usually are not closed components.

In this case, for segmenting Central Sulcus, it is required to close open sides of the Central Sulcus. In the details of Shape Closing part; two different methodology, which is developed to solve this problem, will be explained.

In both of two methodologies, left and right hemisphere handled separately. In other words, same method has been applied for segmentation of left and right sulcus independently.

At the first methodology, region growing has been started from right to left for segmenting left sulcus, on the contrary, left to right for segmenting right sulcus respectively.

For example, for the left sulcus, region growing continued towards left (open side of the left sulcus) iteratively. At every iteration, a new line added to the region and its height has been compared with the average height value, which is recomputed at every iteration, of the Central Sulcus region. If there is a dramatic difference between height of the newly added line and average height value of the Central Sulcus region, algorithm assumes that segmentation leaked into out of brain boundary and stops segmentation. This technique called “Dynamic Height Measuring” method.

At the second methodology, brain masks, which were created using BET, has been used to create a boundary for Central Sulcus. Same as with the previous methodology, every neighbor pixels around seed point clusters were visited and intensity value of those pixels were compared with the cluster’s average intensity value. Differently, in this methodology, a new condition is applied to the pixel by comparing its coordinates with the brain mask. If the brain mask has a positive value at this coordinate, then it is assumed that this pixel belongs to brain tissue and can be added into cluster. After adding this pixel

into cluster, average intensity value recomputed by taking current point's intensity value into account.

In some cases, brain mask image which is generated by BET, may contain over segmented region. Because of the noise or dramatic atrophy in brain, BET algorithm sometimes confuses CSF with the skull or other tissues in the brain. Region growing technique can't detect where to end growing of the region in similar cases. To minimize over segmentation, erosion operation applied on the brain mask.

Erosion is one of the morphological operations can be applied on binary or grayscale images. In erosion, a pre-defined shape (structuring image) is probed over target image iteratively. At every iterating, each component of the structuring image has been compared with the target image, where the structuring image is currently located. If structuring image doesn't fit with the target image, this region removed from the target image.

Both methodologies have advantages and disadvantages in comparison with the other methodologies and studies. This cases will be covered in the "Discussions and Results" section



### **3. RESULTS**

#### **4.1 SLICE SELECTION**

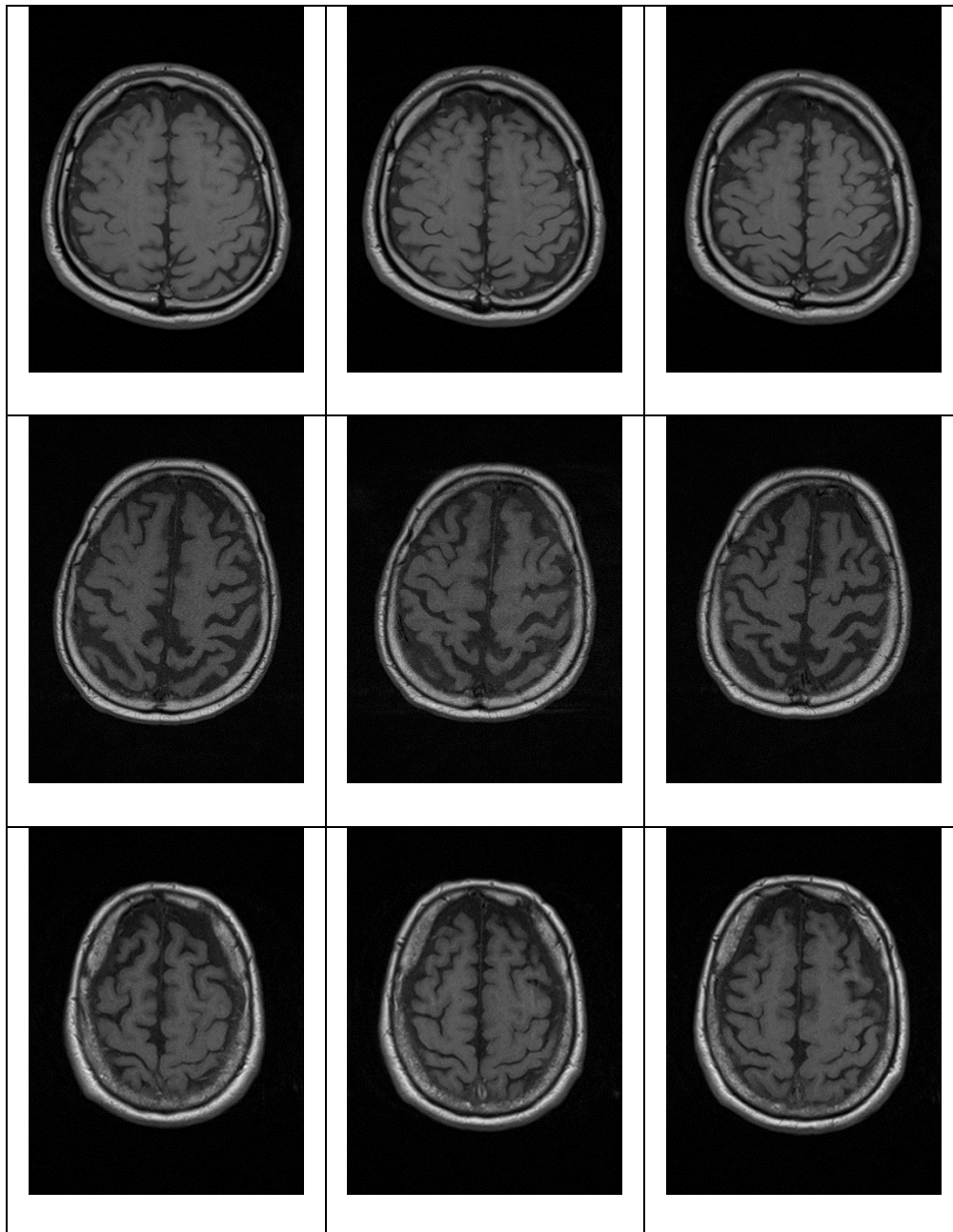
Slice selection is the most important part of this study since it is the starting point of the algorithm. This step finds the key slice which is used as input for the atlas mapping and segmentation phases.

The atlas image that is used in this study, was generated by using key slices of different MR images. First central sulcus regions were segmented manually and then, those results were combined together in order to generate final atlas image. Thus, for the atlas to fit the target image properly, selection of key slice is important, since the atlas image is generated by using keys slices.

The details of the slice selection has been explained in “Slice Selection” topic of the “Methods” chapter. In this chapter, results of the slice selection part will be covered.

The data set, which is used in this study, contains data of both patients who have dementia diseases and healthy individuals. Regarding the data set of patients, grade of the dementia disease and consequently, atrophy level in the MR images vary. In Table 4.1.1, slice selection results for data of both healthy and atrophic brain can be seen.

**Table 4.1.1: Slice Selection Results**



As a note, there is a similarity between this technique and the work of Wei et al. 2008. In Wei et al. 2008, slice selection phase was handled by, first, finding the slice where the AC and PC can be seen. Then the key slice was found by using AC-PC slice as a reference. In the original paper however, it is not clear how the AC and PC regions were detected

but after the detection of the AC-PC slice; key slice was found by applying the formula below.

$$N = \left( \frac{1}{6} * N_{AC-PC} \right) + \left( \frac{2}{5} * N_{TopTissue} \right)$$

In this formulation  $N_{AC-PC}$  is the number of the slice where the AC-PC plane can be seen, and  $N_{TopTissue}$  is the slice number of the last slice where the brain tissue can be seen.

In order to measure the error of the slice selection, we computed the actual distance of the detected slice to the key slice in mm.

In Table 4.1.2 results of the slice selection can be seen.

**Table 4.1.2: Slice Selection Results with Details**

| Data Number | Count of Missed Slices | Slice Count of Image | Error Ratio (in mm.) | Sum of Error Ratio (in mm.) | Standard Deviation |
|-------------|------------------------|----------------------|----------------------|-----------------------------|--------------------|
| 1           | 0                      | 40                   | 0                    | 1.73052                     | 0.087467           |
| 2           | 1                      | 40                   | 0.09                 |                             |                    |
| 3           | 0                      | 40                   | 0                    |                             |                    |
| 4           | 2                      | 40                   | 0.18                 |                             |                    |
| 5           | 1                      | 25                   | 0.144                |                             |                    |
| 6           | 1                      | 25                   | 0.144                |                             |                    |
| 7           | 1                      | 40                   | 0.09                 |                             |                    |
| 8           | 0                      | 40                   | 0                    |                             |                    |
| 9           | 0                      | 40                   | 0                    |                             |                    |
| 10          | 0                      | 40                   | 0                    |                             |                    |
| 11          | 1                      | 40                   | 0.09                 |                             |                    |
| 12          | 1                      | 40                   | 0.09                 |                             |                    |
| 13          | 1                      | 40                   | 0.09                 |                             |                    |
| 14          | 3                      | 35                   | 0.30852              |                             |                    |
| 15          | 0                      | 40                   | 0                    |                             |                    |
| 16          | 0                      | 40                   | 0                    |                             |                    |
| 17          | 0                      | 40                   | 0                    |                             |                    |
| 18          | 2                      | 40                   | 0.18                 |                             |                    |
| 19          | 2                      | 40                   | 0.18                 |                             |                    |
| 20          | 1                      | 25                   | 0.04                 |                             |                    |
| 21          | 2                      | 40                   | 0.05                 |                             |                    |
| 22          | 0                      | 40                   | 0                    |                             |                    |

## 4.2 ATLAS MAPPING

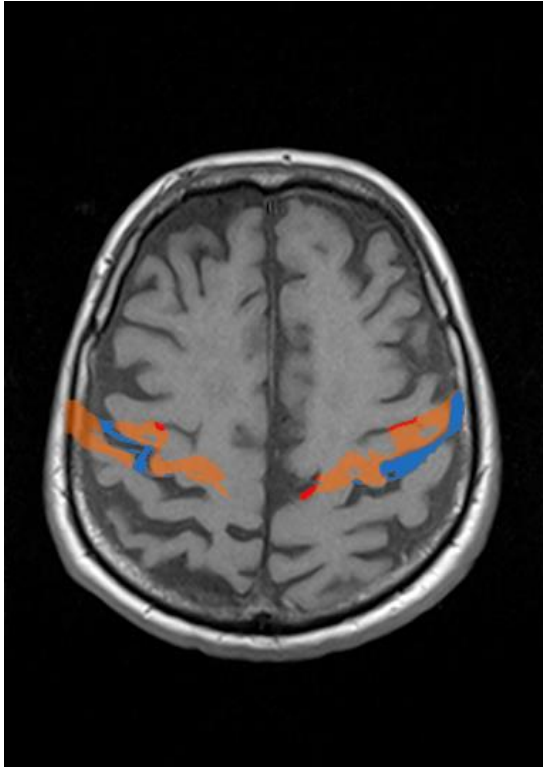
Similar to slice selection, quantifying the success of Atlas Mapping is a tough issue as well.

At the beginning of the process, atlas is generated by combining five different data from patients having different levels of atrophy. In order to generate the atlas image, initially, a target image graded as level-2 (4 is maximum) is selected from within. Then the remaining data is registered over this image by using FLIRT. Key Slices are selected by naked eye and the central sulcus regions are segmented manually. Atlas image is then created by combining all those segmentation results together.

Atlas Mapping, as well as the slice selection phase, directly effects the quality of segmentation. As it is explained earlier in the Methods section, Atlas Mapping technique is used for selecting the seed points for segmentation and locating the Central Sulcus region.

When the first approach was implemented, it is observed that the atlas segmentation map would hit other brain structures (false positives), especially in atrophic brain MR images. In Figure 4.2.2, the aligned atlas can be seen in orange color. The blue and red regions show correct and mismatched intersections between the atlas and the Central Sulcus region.

**Figure 4.2.2: An exemplary visual result of Atlas Mapping**

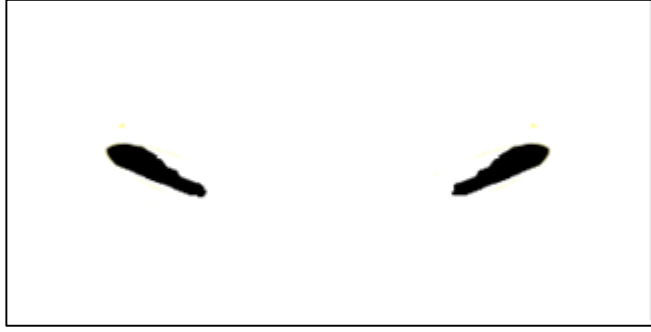


*Red: Mismatched intersection, Blue: Correct intersection, Orange: Atlas region*

In order to minimize such false positives, the atlas is eroded. Although the results were better than those of the previous approach, when this new atlas image was used for mapping there were still errors at the hemispheric fissure region. The reason for this is that the hemispheric fissure becomes dramatically larger at high levels of atrophy. In Figure 4.2.2, this problem can be seen at the MSP level with larger red-marked area.

Finally, the atlas is manipulated in order to fit the orientation of the central sulcus in the key slice. Resulting new atlas image was generated by contracting the central sulcus regions and rotating them by 30 degrees from the horizontal level. Figure 4.2.3 shows the final atlas image.

**Figure 4.2.3: Final Atlas Image**



By using this atlas image, success rate of the atlas mapping is increased dramatically. Central Sulcus region has been detected successfully in 21 of the 22 data.

### 4.3 SEGMENTATION

This section includes results for different approaches which were used in segmentation phase of the algorithm. As it is explained earlier, central sulcus is a fissure and in order to segment this structure, open side of this fissure must be closed. For all the segmentation approaches, same region growing techniques were applied, however different techniques were applied for closing open side of the central sulcus.

In this section, results for those different techniques will be explained. For measurement the dice scoring methodology has been used. Simple formulation of dice scoring can be explained as below:

$$QS = \frac{2C}{A + B} = \frac{2|A \cap B|}{|A| + |B|}$$

Basically, Dice scoring is used to compare two data sets. In this formula, “C” represents number of elements shared in data sets “A” and “B”. In our study, “A” represents the segmentation result of the algorithm, and “B” represents the ground truth data.

In this study, the ground truth data is synthetically generated by manually segmenting central sulcus regions on test data set. After completion of manual segmentation, those data has been approved by a group of neurologists and radiologists from Bayındır

Hospital, İçerenköy. Then, manual segmentation results are exported as binary image stacks in order to be used for evaluation via Dice measure.

In Table 4.3.1, the results for the “Dynamic Height Measuring” method can be seen. As it can be seen in the results, in this technique, usually, open side of the Central Sulcus was closed successfully. Only Data 6 has a 0 Dice score, meaning atlas image was not mapped correctly over image.

**Table 4.3.1: Results for dynamic height measuring**

| <b>Data Reference</b> | <b>Dice Score</b> | <b>Average Dice Score</b> | <b>Standard Deviation</b> |
|-----------------------|-------------------|---------------------------|---------------------------|
| Data 1                | 0.4639            | 0.4305                    | 0.3186                    |
| Data 2                | 0.4591            |                           |                           |
| Data 3                | 0.7156            |                           |                           |
| Data 4                | 0.0000            |                           |                           |
| Data 5                | 0.1054            |                           |                           |
| Data 6                | 0.0000            |                           |                           |
| Data 7                | 0.5638            |                           |                           |
| Data 8                | 0.6582            |                           |                           |
| Data 9                | 0.0000            |                           |                           |
| Data 10               | 0.2756            |                           |                           |
| Data 11               | 0.0327            |                           |                           |
| Data 12               | 0.0635            |                           |                           |
| Data 13               | 0.7990            |                           |                           |
| Data 14               | 0.6971            |                           |                           |
| Data 15               | 0.6688            |                           |                           |
| Data 16               | 0.0242            |                           |                           |
| Data 17               | 0.7227            |                           |                           |
| Data 18               | 0.7982            |                           |                           |
| Data 19               | 0.4275            |                           |                           |
| Data 20               | 0.7517            |                           |                           |
| Data 21               | 0.8128            |                           |                           |

In the second methodology, a brain tissue mask was used to find the open side of the Central Sulcus. Table 4.3.2 displays the results.



**Table 4.3.2: Results for brain masking with BET**

| <b>Data Reference</b> | <b>Dice Score</b> | <b>Average Dice Score</b> | <b>Standard Deviation</b> |
|-----------------------|-------------------|---------------------------|---------------------------|
| Data 1                | 0.8002            | 0.4235                    | 0.2955                    |
| Data 2                | 0.3716            |                           |                           |
| Data 3                | 0.6439            |                           |                           |
| Data 4                | 0.5051            |                           |                           |
| Data 5                | 0.6596            |                           |                           |
| Data 6                | 0.0000            |                           |                           |
| Data 7                | 0.5952            |                           |                           |
| Data 8                | 0.1084            |                           |                           |
| Data 9                | 0.0000            |                           |                           |
| Data 10               | 0.2345            |                           |                           |
| Data 11               | 0.1415            |                           |                           |
| Data 12               | 0.4404            |                           |                           |
| Data 13               | 0.7842            |                           |                           |
| Data 14               | 0.3660            |                           |                           |
| Data 15               | 0.7250            |                           |                           |
| Data 16               | 0.1003            |                           |                           |
| Data 17               | 0.0000            |                           |                           |
| Data 18               | 0.8255            |                           |                           |
| Data 19               | 0.1818            |                           |                           |
| Data 20               | 0.6820            |                           |                           |
| Data 21               | 0.7282            |                           |                           |

In order to improve segmentation quality, erosion operation was applied over the brain tissue mask. Table 4.3.3 displays the results.

**Table 4.3.3: Results for brain masking with erosion operation**

| <b>Data Reference</b> | <b>Dice Score</b> | <b>Average Dice Score</b> | <b>Standard Deviation</b> |
|-----------------------|-------------------|---------------------------|---------------------------|
| Data 1                | 0.6732            | 0.4360                    | 0.2734                    |
| Data 2                | 0.4260            |                           |                           |
| Data 3                | 0.7393            |                           |                           |
| Data 4                | 0.0000            |                           |                           |
| Data 5                | 0.6353            |                           |                           |
| Data 6                | 0.0000            |                           |                           |
| Data 7                | 0.4454            |                           |                           |
| Data 8                | 0.5512            |                           |                           |
| Data 9                | 0.3493            |                           |                           |
| Data 10               | 0.0808            |                           |                           |
| Data 11               | 0.0000            |                           |                           |
| Data 12               | 0.1786            |                           |                           |
| Data 13               | 0.7220            |                           |                           |
| Data 14               | 0.5329            |                           |                           |
| Data 15               | 0.7134            |                           |                           |
| Data 16               | 0.1021            |                           |                           |
| Data 17               | 0.6836            |                           |                           |
| Data 18               | 0.7353            |                           |                           |
| Data 19               | 0.3698            |                           |                           |
| Data 20               | 0.4883            |                           |                           |
| Data 21               | 0.7295            |                           |                           |

To understand effect of the slice selection phase over segmentation results, slice selection was completed manually. Results can be seen in Table 4.3.4

**Table 4.3.4: Results for manual slice selection**

| <b>Data Reference</b> | <b>Dice Score</b> | <b>Average Dice Score</b> | <b>Standard Deviation</b> |
|-----------------------|-------------------|---------------------------|---------------------------|
| Data 1                | 0.6732            | 0.5758                    | 0.1676                    |
| Data 2                | 0.5211            |                           |                           |
| Data 3                | 0.7393            |                           |                           |
| Data 4                | 0.6905            |                           |                           |
| Data 5                | 0.7370            |                           |                           |
| Data 6                | 0.7130            |                           |                           |
| Data 7                | 0.4454            |                           |                           |
| Data 8                | 0.5512            |                           |                           |
| Data 9                | 0.3493            |                           |                           |
| Data 10               | 0.6188            |                           |                           |
| Data 11               | 0.2200            |                           |                           |
| Data 12               | 0.2186            |                           |                           |
| Data 13               | 0.7220            |                           |                           |
| Data 14               | 0.5329            |                           |                           |
| Data 15               | 0.7134            |                           |                           |
| Data 16               | 0.4521            |                           |                           |
| Data 17               | 0.7243            |                           |                           |
| Data 18               | 0.7353            |                           |                           |
| Data 19               | 0.5159            |                           |                           |
| Data 20               | 0.4883            |                           |                           |
| Data 21               | 0.7295            |                           |                           |

Finally, over segmentation regions were manually removed and dice scores re-computed. Results can be seen in Table 4.3.5

**Table 4.3.5: Results for manual slice selection after over segmented regions were removed.**

| <b>Data Reference</b> | <b>Dice Score</b> | <b>Average Dice Score</b> | <b>Standard Deviation</b> |
|-----------------------|-------------------|---------------------------|---------------------------|
| Data 1                | 0.6732            | 0.6105                    | 0.1685                    |
| Data 2                | 0.5211            |                           |                           |
| Data 3                | 0.7802            |                           |                           |
| Data 4                | 0.6905            |                           |                           |
| Data 5                | 0.7370            |                           |                           |
| Data 6                | 0.7130            |                           |                           |
| Data 7                | 0.8254            |                           |                           |
| Data 8                | 0.6712            |                           |                           |
| Data 9                | 0.3493            |                           |                           |
| Data 10               | 0.6188            |                           |                           |
| Data 11               | 0.2200            |                           |                           |
| Data 12               | 0.4145            |                           |                           |
| Data 13               | 0.7407            |                           |                           |
| Data 14               | 0.5329            |                           |                           |
| Data 15               | 0.7134            |                           |                           |
| Data 16               | 0.4521            |                           |                           |
| Data 17               | 0.7243            |                           |                           |
| Data 18               | 0.6732            |                           |                           |
| Data 19               | 0.5211            |                           |                           |
| Data 20               | 0.7802            |                           |                           |
| Data 21               | 0.6905            |                           |                           |

#### 4. DISCUSSIONS AND RESULTS

Automatic segmentation of central sulcus is a hard task since the morphological properties of this structure change from one human individual to the other (due to anatomical and pathological reasons). During this study, different approaches are used for slice selection, atlas generation, atlas mapping, and segmentation the central sulcus.

First of all, it must be said that, the data set we used in this study consists of real cases including a lot of extremes like atrophy, contrast problems, orientation differences, different slice orders etc.

The entire data set is acquired from Bayındır Hospital, İçerenköy and it mostly includes MR images of patients suffering from varying levels of dementia. Depending on this, the brain MR images in the data set includes atrophies, structural deformations and abnormalities. In literature, there are some studies which give results (Sobel et al. 1993) about extreme cases like tumors or other structural abnormalities, however, it can be understood that, these studies deal with the healthy brain MR images since the references to those extreme cases usually take place at discussions session as a note or weakness of the algorithm

Another difficulty about the data set is the variations in the MR images. All the MR images in the data set are in T1-weighted contrast, but there were still extreme contrast differences between the images or noise present in the images. Besides, the slice thickness values vary between 3-7mm. Another major problem about the data was the varying orientations of the images.

Since this study aims to find a full automatic technique for central sulcus segmentation, all of those difficulties were handled automatically in the preprocessing phase of the algorithm.

When this study is compared to the other studies in terms of time efficiency, our only reference is the study of Wei (Wei, 2004). In the result section of the Wei's paper, it has been said that algorithm runs for 15 minutes to identify and segment central sulcus in 3D

space. Our study works in 2D space for now but it finds and segments central sulcus region in 3.2 seconds in average.

This project has been implemented as a standalone ImageJ plugin by using Java programming language. So, it can be installed into ImageJ as a plugin jar file and used by researchers, radiologists or other users. Also, segmentation results can be retrieved as a separate file in Analyze format. Entire project has been tested on both Windows and Mac OS X operating system.

## **5.1 RESULTS**

Slice selection is the most important part of this study since it is used to find the starting point of the rest of the algorithm. All of the steps of the algorithm, other than slice selection, depend on the result of this part indirectly.

In literature, slice selection were referenced in some studies (Wei, 2004) but in the original papers, results of this step have not been included, i.e., it has not been possible to compare slice selection results of this study with the previous works. In this case, only advantages and limitations of the slice selection part of this algorithm can be expressed.

The slice selection technique, which was developed for this study, gives adequate results which can be used for the rest of algorithm. As it is explained in Methods section earlier, slice selection part of the algorithm first finds maximum slice and using an assumption, selects key slice within slices.

There are some limitations and weaknesses in this approach. Success of the slice selection relies on the success of finding maximum slice. Basically, maximum slice is the slice in MR image, which has maximum number of tissue pixels. If the image has too much noise on it, success ratio of finding maximum slice may decrease. Similarly, low contrast in MR image or atrophy in brain tissue may cause difficulties in finding maximum slice.

In MR imaging, there may be angular differences between images. Those angular differences may appear in all planes (sagittal, coronal and axial) caused by the movements of the subject or the way that the image is taken. In some cases, the images cannot be

taken in perpendicular angles because of pathological needs. This algorithm can correct angular differences in axial plane which is resulting from the movement of the subject, by detecting MSP in the brain and rotating the image to the normal angle but cannot correct angular differences caused by the imaging process.

Atlas mapping is the second step of the algorithm. As it is explained earlier, algorithm registers the atlas image over key slice and finds seed points for segmentation. Before mapping atlas over target image, algorithm corrects rotation on Z axis by finding MSP (Ekin, 2006).

The algorithm cannot produce a solution in the case that image is taken upside down (vertically flipped). This may result in atlas to fit different structures of the brain and the results to be completely wrong.

For registering atlas over target image, algorithm starts with finding boundaries of skull by examining brightest voxels in image. Algorithm may fail to find skull in key slice if contrast of the image is not suitable for this task. Also tumors in the brain may cause the algorithm to work improperly while it searches for the skull part of the slice.

In case of high atrophy in brain, atlas image may overlap other sulcal structures or CSF. To eliminate this error, atlas image was contracted by applying erosion morphological operation. Although it is successful in eliminating the error in the data set used in this study, atlas may overlap other brain structures in different data sets.

Region growing technique was used for segmentation of central sulcus in brain. Seed points have been received from atlas mapping phase of the algorithm and regions were constructed by using those points. Then this initial regions were enlarged alongside central sulcus area.

In this study, we had segmentation problems, which are out coming from the nature of MR images. For example; MR images may be extremely noisy. In some cases; noise in the MR image makes it hard to separate brain tissue and CSF. So, region growing algorithm can't work properly and causes over or under segmentation.

Another difficulty which we had in implementation phase of this study was high slice thickness value in Z axis.

High atrophy level in brain may cause the central sulcus to merge with other sulcal structures. As a consequence, segmented region overflows other sulcal structures or CSF and over segmentation occurs.

Since the sulcal structures become larger in mid-level atrophic brain MR images, it is also observed that the region growing technique works better on these images. In region growing, we follow CSF in central sulcus. CSF becomes more visible in atrophic brain images and it makes easy to grow region in central sulcus. Similarly, for atlas mapping, larger seed point regions can be marked alongside central sulcus.

## **5.2 FUTURE WORKS**

This algorithm is implemented to segment central sulcus on 2D space for now. In implementation, key slice has been found within MR image slices and then, region growing technique were applied to segment central sulcus area. Algorithm can produce adequate results in 2D space (single slice) but adding 3D segmentation capabilities may increase the quality of the segmentation results. In some cases, atrophy in the brain, contrast problems or high slice thickness value causes central sulcus not to be able to be traced continuously. In 3D space region growing, central sulcus can be traced through upper and lower slices. Thus, under segmented parts of the central sulcus may be segmented on upper or lower slices.

Additionally, every segmentation result would be used as an atlas for upper and lower slices. It is possible to extract segmentation result of the algorithm as a binary image and convert this image into an atlas image. Then, by using his atlas image in order to segment central sulcus in other slices, it may be possible to extend this algorithm into 3D space.

For the atlas mapping part, as it is early explained, this algorithm fails for the images which were taken vertically flipped. Determination of this type of images and making correction by flipping it vertically, would be another improvement for the algorithm.

This project was implemented as a standalone plugin for ImageJ. ImageJ is an open framework and platform for image processing. It is planned to publicly publish this plugin, in the ImageJ web site, to make it usable by other researchers, radiologists and



users. Also, midsagittal plane detection part of the algorithm can be published as a separate plugin.

It is also planned to document the source codes of this project and publish them as an open source project in near future.

## REFERENCES

### Books

Burger, W., Burke, M.J., 2008. *Digital Image Processing: An Algorithmic Introduction using Java*. Springer.

Tan, P.N., Steinbach, M., Kumar, V., 2006. *Introduction to Data Mining*. Addison-Wesley.

## Periodicals

- Smith, S.M., 2002. Fast robust automated brain extraction. *Human Brain Mapping*. **17**(3), pp. 143-155.
- Jenkinson, M. and Smith, S.M., 2001 A global optimisation method for robust affine registration of brain images. *Medical Image Analysis*. **5**(2), pp. 143-156.
- Jenkinson, M., Bannister, P.R., Brady, J.M. and Smith, S.M., 2002. Improved optimisation for the robust and accurate linear registration and motion correction of brain images. *NeuroImage*. **17**(2), pp. 825-841.
- Inoue T., Shimizu H., Nakasato, N., Kumabe, T. and Yoshimoto, T., 1999. Accuracy and Limitation of Functional Magnetic Resonance Imaging for Identification of the Central Sulcus: Comparison with Magnetoencephalography in Patients with Brain Tumors. *NeuroImage*. **10**, pp. 738-748.
- Shan, Z.Y., Yue, H.G. and Liu, J.Z., 2002. Automated Histogram-Based Brain Segmentation in T1-Weighted Three-Dimensional Magnetic Resonance Head Images. *NeuroImage* **17**, pp. 1587-1598.
- Lohmann, G., 1998. Extracting Line Representations of Sulcal and Gyral Patterns in MR Images of the Human Brain. *IEEE Transactions on Medical Imaging*. **17**(6).
- Goualher, L.G., Procyk, E., Collins, D.L., Venugopal, R., Barillot, C., Evans, A.C., 1999. Automated Extraction and Variability: Analysis of Sulcal Neuroanatomy. *IEEE Transactions on Medical Imaging*. **18**(3).
- Sobel, D.F., Gallen, C.C., Schwartz, B.J., Waltz, T.A., Copeland B., Yamada, S., Hirschkoff, E.C. and Bloom, F.E., 1993. Locating the Central Sulcus: Comparison of MR Anatomic and Magnetoencephalographic Functional Methods. *AJNR*. **14**, pp. 915-925.

## **Others**

Hayashi, N., 2010. Development of identification of the central sulcus in brain. *Radiol Phys Technol.*

Jenkinson, M., Pechaud, M., and Smith, S., 2005. BET2: MR-based estimation of brain, skull and scalp surfaces. *In Eleventh Annual Meeting of the Organization for Human Brain Mapping.*

Wei, Z., 2004. Identification and Segmentation of the Central Sulcus From Human Brain MR Images.

Behnke, K.J., 2008. Automatic classification of sulcal regions of the human brain cortex using pattern recognition.

## CURRICULUM VITAE

**Name Surname:** Oguz Demir

**Address:** Haci Emin Efendi Sok. No:7/5 Tesvikiye / Istanbul

**Date and Place of Birth:** Istanbul – 27.07.1980

**Foreign Language:** English

**Elementary Education:** Yildirim Beyazit Ilkogretimokulu, 1992

**Secondary Education:** Yildirim Beyazit Ilkogretimokulu

**Undergraduate Education:** Mimar Sinan Fine Art Academy, 2002

**Graduate Education:** Bahcesehir University, Present

**Name of Institute:** Graduate School Of Natural And Applied Sciences

**Name of Program:** Computer Engineering

**Work Experience:**

- Bilkom A.Ş. – Developer – 1999-2000
- HSBC Turkey – Ssystem Engineer – 2000 – 2001
- IS Investment – Assistan Manager – 2001 – 2010
- Terra – Owner – 2010 – Present